Liquid film modeling in high shear nozzles

By W.-W. Kim †, S. Apte, M. Herrmann AND F. Ham

As part of the ongoing development of predictive simulation capabilities for jet engine combustors, two approaches for modeling liquid film formation and evolution in the context of high shear nozzles are investigated. In the first approach, the dense spray region and liquid film formation is modeled by closely packed droplets moving in layers. It is shown that the displacement of gas-phase by droplet finite-size effects can capture the spreading of the liquid film on the injector walls. Collision dominates in the near wall region and is captured using an inter-particle stress model. In the second approach, a transport equation for film-height based on the lubrication theory is solved near the wall. The droplets are represented by the dense spray model until they hit the wall. After impingement, the Lagrangian droplet/parcel is removed and its mass and momentum are transferred to evolve the film-height. We perform a preliminary assessment of these models for two configurations: a liquid jet impinging vertically on a flat plate and a simplified injector consisting of a turbulent channel flow with spray impinging onto one of the channel walls.

1. Introduction

1.1. *Problem Description*

Modern aero-engine gas turbine combustors employ high shear nozzles to atomize liquid fuel as it enters the combustion chamber. Figure 1 shows a schematic of a high shear nozzle, and illustrates the processes that lead to the final distribution of fuel droplets in the downstream combustion chamber. Fuel is introduced through a small number of radial jets near the center of the nozzle. Instabilities created by the interaction of high shear rates with the liquid column lead to an almost immediate stripping of small droplets from the surface of the jet as it penetrates into the swirling crossflow. The core column remains largely intact, however, and undergoes breakup later at a characteristic length scale L_B (figure 2).

For certain nozzle designs, the breakup length scale L_B can be longer or significantly longer than the nozzle dimensions, and the liquid column impinges on an inner nozzle wall, forming a liquid film. This film interacts with the turbulent boundary layer, eventually leaving the front of the nozzle where it undergoes breakup as it interacts with an additional swirling airflow (figure 3).

1.2. *Simulation Challenges*

Prediction of droplet size-distributions and size-velocity correlations produced by high shear nozzles plays a crucial role in accurately modeling the dynamics of spray flames, pollutant formation and emissions. While the various physical processes described in the previous subsection are reasonably well understood, the direct numerical simulation of the atomization process remains excessively costly because most of the breakup occurs at

† Pratt & Whitney

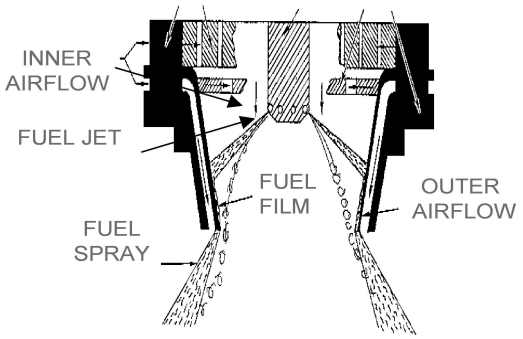

FIGURE 1. Schematic of a high shear nozzle illustrating the liquid fuel breakup and atomization process.

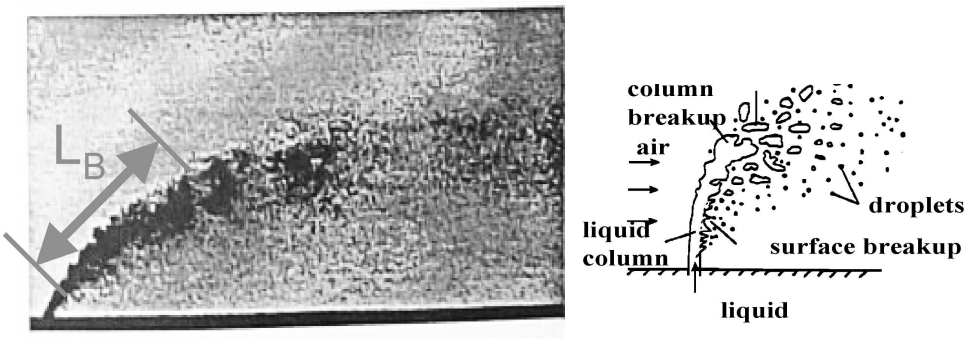

FIGURE 2. Experimental results and schematic illustrating liquid jet breakup process.

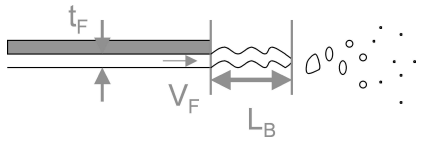

FIGURE 3. Characteristic scales associated with the film breakup process.

length and time scales significantly smaller than those that can be resolved on reasonable computational grids. Consequently subgrid modeling must be used.

In the present investigation, we investigate models for just the liquid film formation and evolution component of the breakup process. While this may seem excessively restrictive, it is expected that a film model can readily be integrated with the existing stochastic breakup models in the LES code CDP (Mahesh *et al.* 2004; CITS report 2004), and used to provide an initial condition (velocity, length scale, and azimuthal distribution) for the Lagrangian point particles/parcels that presently model the disperse liquid phase in the combustion chamber (Apte *et al.* 2003c; Apte *et al.* 2003a).

2. Modeling Approaches and Results

2.1. *Approach 1: Dense Spray Model*

In this model, the liquid phase is solved in the Lagrangian framework and the carrier or fluid phase in the Eulerian framework. The liquid film is represented by a layer of droplets

flowing together. The important differences between this model and the standard point-particle approach employed for two-phase flows (Apte *et al.* 2003c) are: 1) the inter-particle distances are small and liquid flow is collision dominated, 2) the local liquid-phase volume fraction is large and the standard drag-laws need modification, 3) the carrier fluid is treated as a mixture of liquid and gaseous phases and the continuity and momentum equations as well as properties such as viscosity are modified by the volume fraction. This formulation for dense sprays was first derived by Dukowicz (1980) and also proposed by Joseph & Lundgren (1990) for dense particulate flows. The details of this formulation and its implementation on unstructured grids to simulate dense particulate flows is discussed by Apte *et al.* 2003b. We apply this model to simulate liquid film formation and dense spray regimes in gas-turbine combustors. In addition, this model will be used in the second approach described later to track droplets till they hit a wall and form a liquid film.

In the present work, we focus on the first two parts of the model: viz., inter-droplet collisions and modifications to drag forces experienced by droplets. First we neglect the important effect of fluid displacement due to the presence of droplets, however, prevent overlapping of droplet centroids through the collision model. The effect of dense liquid phase is then indirectly captured through two-way coupling between the two phases. Note that in standard point-particle approach where collisions are neglected, the droplets could overlap and may not be able to sustain a layer of droplets flowing together.

The liquid volume fraction Θ_p is defined as,

$$\Theta_p(\mathbf{x}) = \sum_{k=1}^{N_p} V_k \mathcal{G}_\sigma\left(\mathbf{x} - \mathbf{x}_{\mathbf{p}k}\right) \tag{2.1}$$

where the summation is over all particles N_p. Here $\mathbf{x}_{\mathbf{p}k}$ is the particle location, $\mathbf{x}$ centroid of a control volume, and V_k the volume of a particle. The function $\mathcal{G}_\sigma$ is the interpolation operator given as

$$\mathcal{G}_\sigma(\mathbf{x}_p) = \frac{1}{(\sigma\sqrt{2\pi})^3} exp\left[\frac{-(x-x_p)^2 + (y-y_p)^2 + (z-z_p)^2}{2\sigma^2}\right] \tag{2.2}$$

The resulting Θ_p will be smooth and mass-conserving provided $\mathcal{G}_\sigma$ is smooth. A Gaussian interpolation function with filter-width (σ) proportional to grid size and satisfying $\int_V \mathcal{G}_\sigma\left(\mathbf{x} - \mathbf{x}_{\mathbf{p}k}\right) dV = 1$ is used.

The liquid phase equations for individual droplets in Lagrangian framework are,

$$\frac{d}{dt}(\mathbf{x}_p) = \mathbf{u}_p \tag{2.3}$$

$$m_p \frac{d}{dt}(\mathbf{u}_p) = F_p = m_p \mathbf{a}_p \tag{2.4}$$

The total force on a particle consists of the standard hydrodynamic drag force, dynamic pressure gradient, gradient of viscous stress in the fluid phase, a generalized buoyancy force, and inter-particle collision. For the present spray application, the density ratio ρ_p/ρ_f is large ($\approx 10^3$), and we neglect the pressure gradient, viscous stress and buoyancy forces, the total acceleration of the particle $\mathbf{a}_p$ is given as

$$\mathbf{a}_p = \frac{(\mathbf{u}_g - \mathbf{u}_p)}{\tau_r} + \mathbf{a}_{coll} + \left(1 - \frac{\rho_f}{\rho_p}\right)\mathbf{g} \tag{2.5}$$

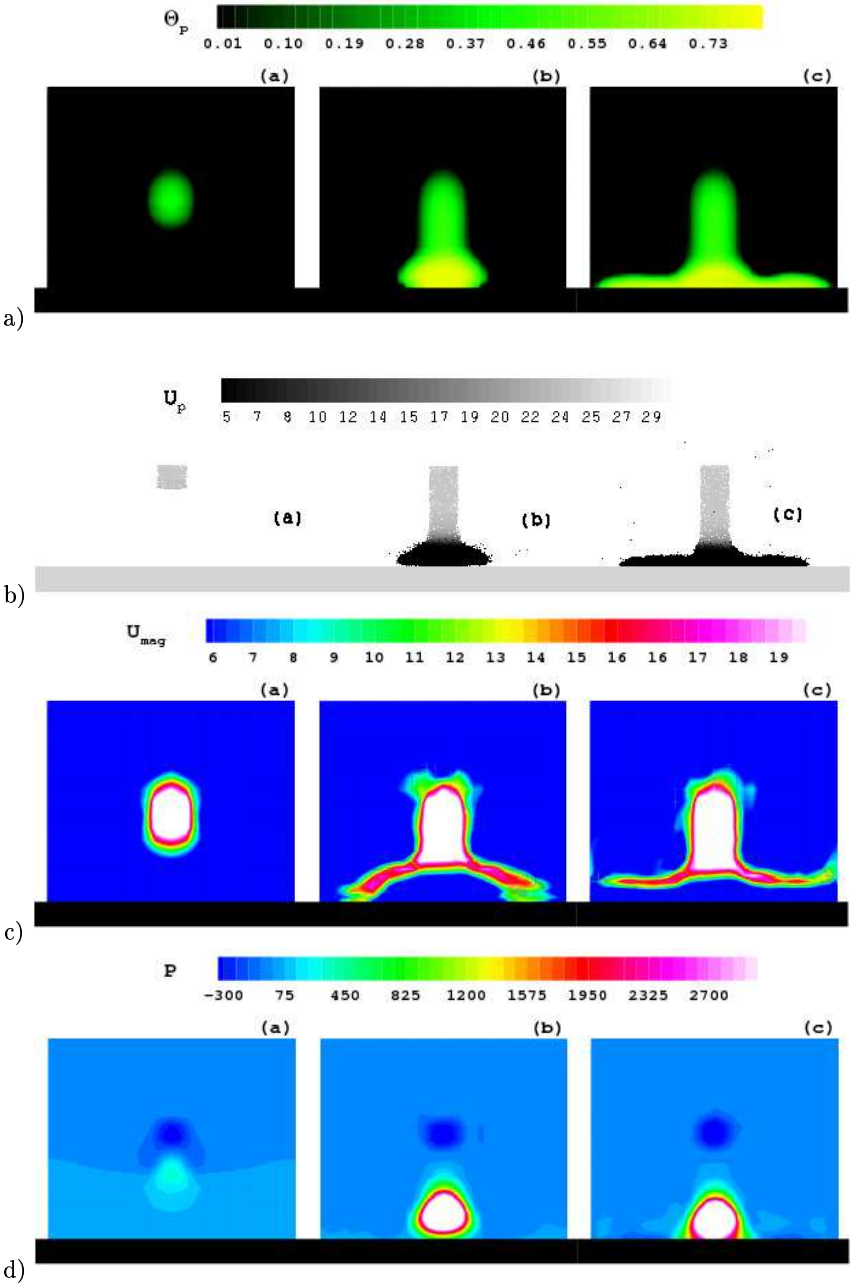

FIGURE 4. Temporal evolution of film formation in direct impact of liquid spray onto a flat plate. Liquid spray is represented by discrete particles of same density. Particles initially clustered at the top move vertically down, impact the flat plate and build up. Particle build up opposes incoming particles, creates a stagnation point, develops a strong gas-phase velocity field through two-way coupling and spreads the film. The present computation includes only the collision model keeping the particle centroids from overlapping each other. (*a*): Particle volume fraction, (*b*): particle positions color coded with particle velocity magnitude, (*c*): gas-phase velocity magnitude, (*d*): pressure.

The drag force is caused by the motion of a particle through the gas. The standard expression for τ_r, the particle relaxation time is

$$\frac{1}{\tau_r} = \frac{3}{8} C_d \frac{\rho_g}{\rho_p} \frac{|\mathbf{u}_g - \mathbf{u}_p|}{R_p} \tag{2.6}$$

where C_d is the drag coefficient and is dependent on the particle Reynolds number, volume fraction and viscosity given by Andrews & O'Rourke (1996).

$$C_d = \frac{24}{Re} \left(1 + a Re_p^b\right) \Theta_g^{-1.8}, \quad for \quad Re_p < 1000 \tag{2.7}$$

$$= 0.44 \Theta_g^{-1.8}, \quad for \quad Re_p \geq 1000 \tag{2.8}$$

where C_d is the drag coefficient for spherical particles, $R_p = (3V_p/4\pi)^{1/3}$ is the particle radius. The particle Reynolds number (Re_p) is given as

$$Re_p = \frac{2\rho_g \Theta_g |\mathbf{u}_g - \mathbf{u}_p| R_p}{\mu_g}. \tag{2.9}$$

There is an indirect collective effect in this drag term: when there is a dense collection of particles passing through the fluid interphase momentum exchange term will cause $\mathbf{u}_g$ to approach the particle velocity, $\mathbf{u}_p$ thus decreasing the drag on a particle, a drafting effect. The acceleration of particles due to inter-particle interactions ($\mathbf{a}_{coll}$) is an important term in dense sprays. A simple model for acceleration of particles due to collision ($\mathbf{a}_{coll}$) is

$$\mathbf{a}_{coll} = -\frac{1}{\Theta_p \rho_p} \bigtriangledown \tau \tag{2.10}$$

where τ is the interparticle stress that provides a pressure type force that prevents packing of particles beyond the close-packing limit. Expression for τ is given as (Harris & Crighton (1994))

$$\tau = \frac{P_s \Theta_p^\beta}{\Theta_{cp} - \Theta_p} \tag{2.11}$$

where P_s has units of pressure, Θ_{cp} is the particle volume fraction at close packing and β is a constant. Here it is assumed that the droplets are rigid spheres and thus there exists a close-packing limit beyond which the droplets would not remain spherical nor rigid. The values for P_s and β are obtained from Andrews & O'Rourke (1996). In this model, the inter-particle acceleration due to particle collision is assumed to be independent of its size and velocity. This model is least expensive in terms of computational cost as particle binary pairs are not formed and the collision force is directly obtained by interpolation from equation (2.10). It should be noted that, this model cannot accurately represent collision between two individual droplets, however, does represent collective behavior of a cluster of droplets and their collisions with others.

Finally, the force on the gas-phase through two-way coupling is given as

$$F(\mathbf{x}, \mathbf{t}) = -\frac{\mathbf{1}}{V} \sum_{\mathbf{x_p} \mathbf{in} V(\mathbf{x})} \mathbf{F_p} \tag{2.12}$$

It should be noted that, in dense spray regime, the liquid mass loading is large and the total force acting on the carrier phase could become large. An explicit treatment of this force gives rise to stability problems in the solution of carrier-phase momentum equations. Owing to this difficulty, in many simulations of practical combustors with dense spray

regimes and liquid atomization, the two-way coupling effects are often neglected. This, however, may give erroneous evolution of the spray near the injector. In order to overcome this difficulty, we implemented an implicit coupling for the drag force.

In brief, the algorithm is as follows: 1) advance the droplet centroids explicitly, 2) compute the volume fraction fields and inter-particle collision forces based on the new droplet locations, 3) represent the carrier-phase velocity interpolated at the particle location in equation 2.6 implicitly and solve the carrier phase equations using a fractional step algorithm on unstructured grids (Mahesh *et al.* 2004), 4) knowing the new velocity field of the carrier phase advance the droplet velocities, 5) recompute the total drag on droplets and correct the carrier-phase velocity fields as a third fractional step using any residual force to discretely conserve momentum transfer between the two phases. In this algorithm, the collision force acting on the droplets is represented explicitly and gives time-step restrictions in advancing the droplet equations. However, the time-steps generally employed in LES do not move the droplets by more than 2-3 times their diameters in one iteration and thus the time-step restriction from the collision model is not severe. The advancement of droplet positions can be made more accurate by sub-dividing the time-step into tiny steps and recomputing the collision force in each sub-step.

Figure 4 shows the results obtained from the dense-spray model for impingement of a liquid jet onto a flat plate. In this model problem, there is no initial gas-phase flow over the flat plate. Liquid jet impinges vertically and spreads to form a film. Here the liquid jet is modeled as a collection of closely packed particles of same density as the liquid. As a first approximation, the particles are assumed as rigid spheres. These particles have an initial velocity of 25 m/s in the vertical direction. They impinge the flat plate and undergo a plastic collision losing all of their normal momentum. A stack of particles builds near the boundary. These stagnant particles oppose the incoming particles through the collision model and spread them in the horizontal plane. The strong momentum coupling between the two-phases creates a velocity field (Fig. 4c) and a pressure field (Fig. 4d). Formation and growth of the liquid film is clearly observed. We plan to perform a detailed validation study of the model and use it for prediction of spray size distributions in a new injector designed by Pratt & Whitney.

Approach 2: Thin Film Model

In this second approach, the liquid film formed by the impact of a fuel spray onto the nozzle walls is treated as a thin film. Introducing the lubrication approximations for thin films into the Navier-Stokes equations, an equation for the evolution of the film height h above a no-slip wall can be derived (Oron *et al.* 1997),

$$\frac{\partial h}{\partial t} + \nabla_1 \cdot \left[\frac{1}{2} h^2 \boldsymbol{\tau}_g + \frac{1}{3} h^3 \nabla_1 \left(N_g - \frac{\mathrm{Re}}{\mathrm{Fr}^2} h + \frac{1}{C} \nabla_1^2 h \right) \right] = 0 \,. \tag{2.13}$$

Here, $\boldsymbol{\tau}_g$ and N_g are the tangential respectively normal stresses exerted by the outside gas onto the liquid film surface, cp. Fig. 5, Re and Fr are the Reynolds and Froude number, ∇_1 is the Nabla-operator in the x-y-wall coordinate system, and C is the capillarity number,

$$C = \frac{u_0 \mu_l}{\sigma} \,, \tag{2.14}$$

with u_0 a reference velocity, μ_l the liquid viscosity, and σ the surface tension coefficient.

To include the effect of the impinging spray, (2.13) has to be extended by appropriate source terms. Assuming, as an initial step, that all drops coming into contact with the

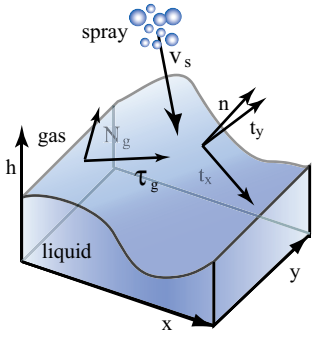

FIGURE 5. Film definition

film surface are fully absorbed into the film such that no splashing occurs, the impinging spray constitutes a mass respectively height source q_s,

$$q_s = \frac{\dot{m}_s}{\rho_l \Delta A}\,, \tag{2.15}$$

where $\dot{m}_s$ is the mass flux of the impinging spray, ρ_l is the liquid density, and ΔA is the size of the wall grid cell where impingement occurs. The inclusion of a detailed splashing model is straightforward and will be considered in the future. Besides its mass, each absorbed drop transfers its momentum to the film. Here, we assume that all momentum is transferred to the film within the single grid cell where absorption occurs. This results in additional normal and tangential stresses,

$$N_s = \mathrm{Re}\,\frac{(m\boldsymbol{v})_s}{\delta t_I \Delta A} \cdot \boldsymbol{n} \tag{2.16}$$

$$\boldsymbol{\tau}_s = \mathrm{Re}\,\frac{(m\boldsymbol{v})_s}{\delta t_I \Delta A} \cdot \boldsymbol{t}\,, \tag{2.17}$$

with $(m\boldsymbol{v})_s$ the impacting spray momentum, $\boldsymbol{n}$ and $\boldsymbol{t}$ the film surface normal and tangential vector, cp. Fig. 5, and δt_I an impact time scale.

Including all spray impingement effects, the evolution equation for the film height then reads

$$\frac{\partial h}{\partial t} + \nabla_1 \cdot \left[\frac{1}{2}h^2\left(\boldsymbol{\tau}_g + \boldsymbol{\tau}_s\right) + \frac{1}{3}h^3\nabla_1\left(N_g - \frac{\mathrm{Re}}{\mathrm{Fr}^2}h + N_s + \frac{1}{C}\nabla_1^2 h\right)\right] = q_s\,. \tag{2.18}$$

Finally, the effect of the liquid film on the outer flow field has to be taken into account by modifying the respective boundary conditions. First, the boundary conditions have to be moved a distance of h away from the wall, and second, the usual no-slip velocities have to be replaced by the film surface velocities,

$$\boldsymbol{v}^{CDP} = \boldsymbol{n} \cdot w_h + \boldsymbol{t} \cdot \boldsymbol{v}_{t,h}\,, \tag{2.19}$$

with

$$\boldsymbol{v}_{t,h} = h\boldsymbol{\tau}_g + \frac{1}{2}\nabla_1 \cdot \left(N_g - \frac{\mathrm{Re}}{\mathrm{Fr}^2}h + N_s + \frac{1}{C}\nabla_1^2 h\right)h^2 \tag{2.20}$$

and

$$w_h = \frac{\partial h}{\partial t} + \boldsymbol{v}_{t,h} \cdot \nabla_1 h\,. \tag{2.21}$$

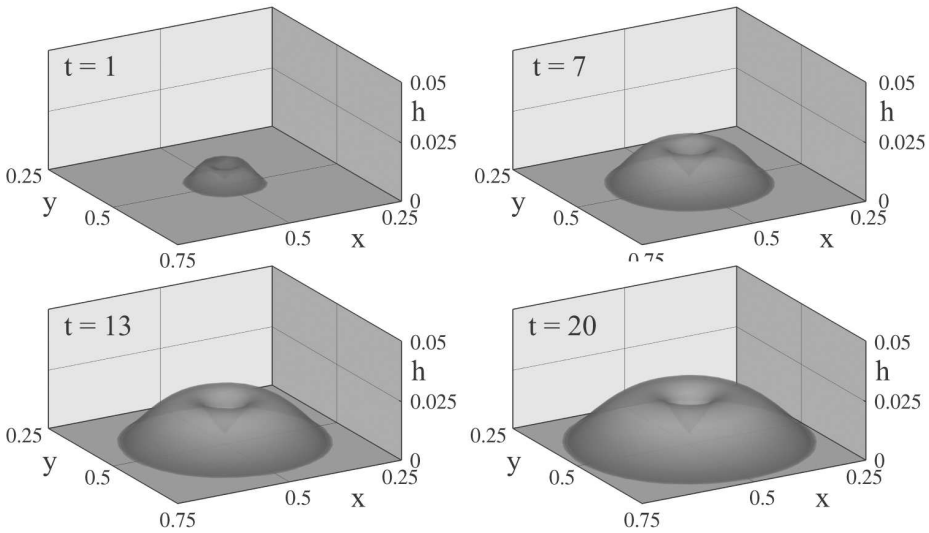

FIGURE 6. Spreading of a film on a flat plate

2.1.1. *Numerical method*

The film equation, (2.18), constitutes a fourth order PDE with a stable time step restriction of

$$\Delta t_h = \min\left(\alpha_1 \frac{\Delta x_{\min}}{|\boldsymbol{\tau}_g + \boldsymbol{\tau}_s|_{\max} h_{\max}}, \alpha_2 \frac{C\Delta x_{\min}^4}{h_{\max}^3}, \alpha_2 \frac{C\Delta x_{\min}^3}{h_{\max}^2}, \alpha_3 \frac{1}{|q_s|_{\max}}, \alpha_4 \frac{\Delta x_{\min}}{\max\left(\partial N/\partial x, \partial N/\partial y\right) h_{\max}^2}\right), \tag{2.22}$$

where α_i are CFL numbers of order 1. Since, in the worst case, $\Delta t_h \sim \Delta x^4$, severe time step restrictions can be imposed on an explicit solver, usually necessitating the use of an implicit solver. However, since (2.18) is incorporated into CDP, the CPU time spent to solve the film equation on a typical CDP grid employing an explicit solver is negligible compared to the CPU time spent in a single CDP time step. This is due to the fact that (2.18) is only two-dimensional.

In practice, (2.18) is solved on a separate, two-dimensional wall grid, using a first order upwind scheme for the advection term involving the tangential stresses and a positivity preserving scheme (Diez & Kondic 2002) employing central differences for all higher order terms. Integration in time is first order. Bilinear interpolation is used to transfer quantities from the wall grid to the CDP grid and vice versa. However, (2.19) has been neglected for now.

To capture the spreading of the film on the underlying wall, a precursor film model is employed (de Gennes 1985; Troian *et al.* 1989). This circumvents the explicit treatment of contact line angles and thereby avoids any contact line singularities.

2.1.2. *Thin Film Model Results*

The implementation of the film equation has been verified comparing the numerical solutions of traveling surface waves under shear stress to analytical solutions. The obtained results show excellent agreement with the theory.

To demonstrate the performance of the film model in the combustor code CDP, the

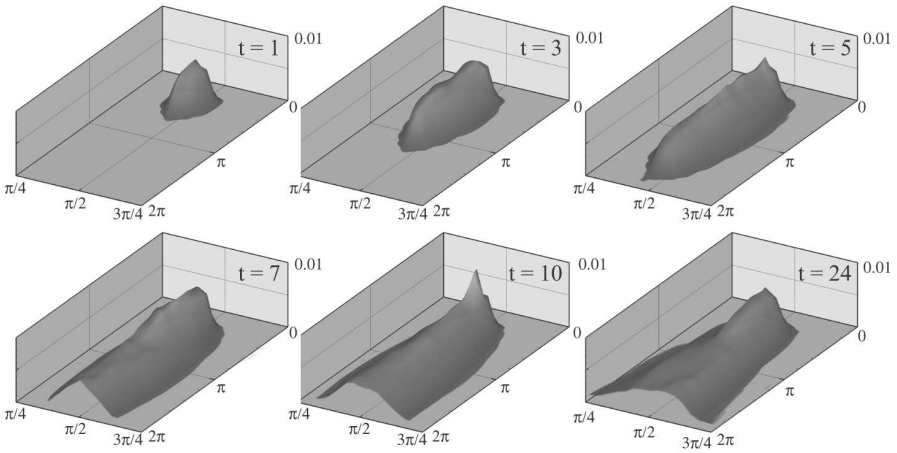

FIGURE 7. Spreading of a film in a turbulent channel

results of two different example cases are presented in the following. In the first case, a spray with density $\rho_l = 850\,\mathrm{kg/m^3}$ and $\dot{m} = 1\,\mathrm{kg/s}$ impacts vertically onto a $1\,\mathrm{m}^2$ square flat plate in a square area of $16\,\mathrm{cm}^2$ located at the center of the plate. The spray is injected just above the film, so that the momentum coupling between the spray and the gas-phase can be neglected. The capillarity number is $C = 0.018$, the Reynolds number $\mathrm{Re}_s = 9700$, and the Froude number $\mathrm{Fr} = 0.023$. Figure 6 shows the spreading of the developing film. The effect of the momentum transfer from the spray to the film is clearly visible in the impact area, where the film is visibly depressed. As time progresses, the film starts to spread and forms a circular wetting area, resulting in a maximum film height of roughly 2 mm.

In the second example, a spray with $\dot{m} = 10.9\,\mathrm{g/s}$ is injected in a 45^o angle onto a $2\pi \times \pi$ sized wall of a turbulent channel with Reynolds number $\mathrm{Re} = 395$. The capillarity number is $C = 0.25$, the film Reynolds number $\mathrm{Re} = 1.3 \cdot 10^5$, and the Froude number $\mathrm{Fr} = \infty$. To highlight the effect of the outside flow field on the film evolution, the gas-phase stresses acting on the film surface have been enhanced by a factor of 100. Figure 7 shows the evolution of this film. After the initial impact, the film is quickly pushed along the channel wall by the outside gas-phase flow and starts to spread in the transverse direction. Note that due to the turbulent fluctuations of the gaseous shear stresses, fluctuations in the film height are generated.

3. Conclusions

Two approaches for modeling liquid film formation and evolution in the context of high shear nozzles have been implemented in the unstructured LES code CDP. Both approaches show promise in describing the physics of film formation and evolution, and its impact on the gas phase. As part of an ongoing collaboration with Pratt & Whitney, both models will be validated against cold-flow experimental data in a test rig configuration involving a high shear nozzle. Depending on the results of this validation, one or both approaches will then be used to perform a pre-test prediction of an experimental combustor configuration scheduled for detailed cold and hot flow measurements in early 2005.

REFERENCES

ANDREWS, M. J., & O'ROURKE, P. 1996 The multiphase particle-in-cell (MP-PIC) method for dense particle flow. *Int. J. Mult. Flow* **22**:379–402.

APTE, S. V., GOROKHOVSKI, M. & MOIN, P. 2003a LES of atomizing spray with stochastic modeling of secondary breakup. *Int. J. Mult. Flow* **29**:1503-1522.

APTE, S. V., MAHESH, K., & LUNDGREN, T. 2003b An Eulerian-Lagrangian model to simulate two-phase/particulate flows. *Annual Research Briefs*, Center for Turbulence Research, Stanford University.

APTE, S. V., MAHESH, K., MOIN, P. & OEFELEIN, J. C. 2003c LES of swirling particle-laden flows in a coaxial-jet combustor. *Int. J. Mult. Flow* **29**:1311–1331.

CITS Annual technical report 2004. *Center for Integrated Turbulence Simulations, Stanford University.*

DIEZ, J.A., AND KONDIC, L. 2002 Computing three-dimensional thin film flows including contact lines. *J. Comput. Phys.* **183**:274–306.

DUKOWICZ, J. K. 1980 A particle-fluid numerical model for liquid sprays. *J. Comput. Phys.* **35**:229–253.

DE GENNES., P. G. 1985 Wetting: Statistics and dynamics. *Rev. Mod. Phys.* **57**:827–863.

HARRIS, S.E., & CRIGHTON, D.G. 1994 Solutions, solitary waves and viodage disturbances in gas-fluidized beds. *J. Fluid Mech.* **266**:243–276.

JOSEPH, D.D., & LUNDGREN, T. 1990 Ensemble averaged and mixture theory equations for incompressible fluid-particle suspensions. *Int. J. Mult. Flow* **16**:35–42.

MAHESH, K., CONSTANTINESCU, G. & MOIN, P. 2004 A numerical method for large-eddy simulation in complex geometries. *J. Comput. Phys.* **197**:215–240.

ORON, A., DAVIS, S. H., AND BANKOFF, S. G. 1997 Long-scale evolution of thin liquid films. *Rev. Modern Phys.*, **69**(3):931–980.

TROIAN, S. M., HERBOLZHEIMER, E., SAFRAN, S. A., AND JOANNY, J. F. 1989 Fingering instabilities of driven spreading films. *Europhys. Lett.* **10**:25–30.